

# VEPSD: A Novel Velocity Estimation Algorithm for Next-Generation Wireless Systems

Shantidev Mohanty, *Student Member, IEEE*

**Abstract**—A novel algorithm called velocity estimation using the power spectral density (VEPSD), which uses the Doppler spread in the received signal envelope to estimate the velocity of a mobile user (MU), is introduced in this paper. The Doppler spread is estimated using the slope of the power spectral density (PSD) of the received signal envelope. The performance of the VEPSD algorithm is evaluated in both Rayleigh and Rician fading environments. The sensitivity of the estimation error to additive white Gaussian noise (AWGN), Rice factor ( $K$ ), and the angle of arrival of the line-of-sight (LOS) component is analyzed and compared with the level crossing rate (LCR) and covariance-based velocity estimators. Simulation results show that VEPSD estimates the velocity of MUs accurately. It is also shown that VEPSD can be used for velocity estimation under nonisotropic scattering and is well suited for next-generation wireless systems (NGWSs).

**Index Terms**—Doppler spread, fading environments, next-generation wireless systems (NGWSs), power spectral density, velocity estimation.

## I. INTRODUCTION

IN CURRENT and next-generation wireless systems (NGWSs), the estimation of users' velocity<sup>1</sup> is important to improve the network performance. In hierarchical cellular systems, the velocity information can be used to assign slow-moving users to micro/picocells and fast-moving users to macrocells to reduce the handoff rate for the fast-moving users. This increases the system capacity and reduces the number of dropped calls [1]. Moreover, velocity information can be used to ensure successful handoff in a cellular system. For example, when the position and the velocity of a mobile user (MU) is known, MU's arrival time in the next cell can be estimated and, accordingly, resources can be reserved in advance to ensure a successful handoff.

Several techniques are proposed in the literature for velocity estimation. The algorithm proposed in [1] using the normalized autocorrelation values of the received signal is efficient in classifying the velocity into slow, medium, or fast. However, a better resolution of the velocity is not achievable. In [2], the level crossing rate (LCR)-based velocity estimator is proposed. However, in the presence of additive white Gaussian noise (AWGN), this estimator suffers from severe estimation error when the

velocity is low. Wavelets are used in [3] for velocity estimation. Switching rate of diversity branches is used for the velocity estimation in [4], but it is shown in [5] that this method is sensitive to the fading scenarios. Hence, it is not practical. In [6], velocity estimation algorithms that use pattern recognition are proposed. However, these algorithms are computationally intensive [1]. In [7], a velocity estimator based on the statistical analysis of the channel power variations is proposed. In [8], the squared deviations of the received signal envelope is used for velocity estimation. Adaptive array antennas are used for the velocity estimator proposed in [9]. The first moment of the instantaneous frequency of the received signal is used in [12] for the velocity estimation. However, this study is limited only to the Rayleigh fading channels.

A coarse estimation that classifies velocity to slow, medium, or fast is sufficient when the velocity information is used to assign an MU to a macro-, micro-, or picocell. On the other hand, accurate velocity estimation is required for seamless mobility support [13] in NGWS. Hence, the desired accuracy of velocity estimation depends on the application. Moreover, the accuracy of velocity estimation should be independent of the fading types (e.g., Rayleigh and Rician fading). Finally, the algorithm should not be computationally extensive. To our knowledge, none of the existing velocity estimation techniques mentioned above satisfy all these requirements simultaneously.

In this paper, we propose a novel algorithm called VEPSD for velocity estimation. In VEPSD, we first estimate the maximum Doppler spreading frequency ( $f_m$ ). Then, we use  $f_m$  for velocity estimation. VEPSD satisfies the above-mentioned requirements of an efficient velocity estimation algorithm.

The rest of this paper is organized as follows. In Section II, we provide a detailed description of the proposed VEPSD algorithm. We present the performance evaluation of VEPSD in Section III. Finally, we summarize the performance and advantages of VEPSD algorithm in Section IV.

## II. VEPSD

The maximum Doppler frequency ( $f_m$ ) is related to the velocity ( $v$ ) of an MU, speed of light in free space ( $c$ ), and the carrier frequency ( $f_c$ ) through

$$v = \left( \frac{c}{f_c} \right) f_m. \quad (1)$$

In case of a narrowband multipath fading channel, the received low pass signal is given by

$$r(t) = \sum_{n=1}^N \alpha_n e^{j\beta_n} e^{(j2\pi f_m \cos \theta_n)t} + w(t) \quad (2)$$

Manuscript received November 23, 2003; revised September 30, 2004; accepted December 22, 2004. The editor coordinating the review of this paper and approving it for publication is N. Mandayam. This work was supported by the National Science Foundation under Project ANI-0117840.

The author is with the Broadband and Wireless Networking Laboratory, School of Electrical and Computer Engineering, Georgia Institute of Technology, Atlanta, GA 30332 USA (e-mail: shanti@ece.gatech.edu).

Digital Object Identifier 10.1109/TWC.2005.858300

<sup>1</sup>Velocity is a vector with both magnitude and direction. However, we refer to the magnitude as the velocity throughout this paper.

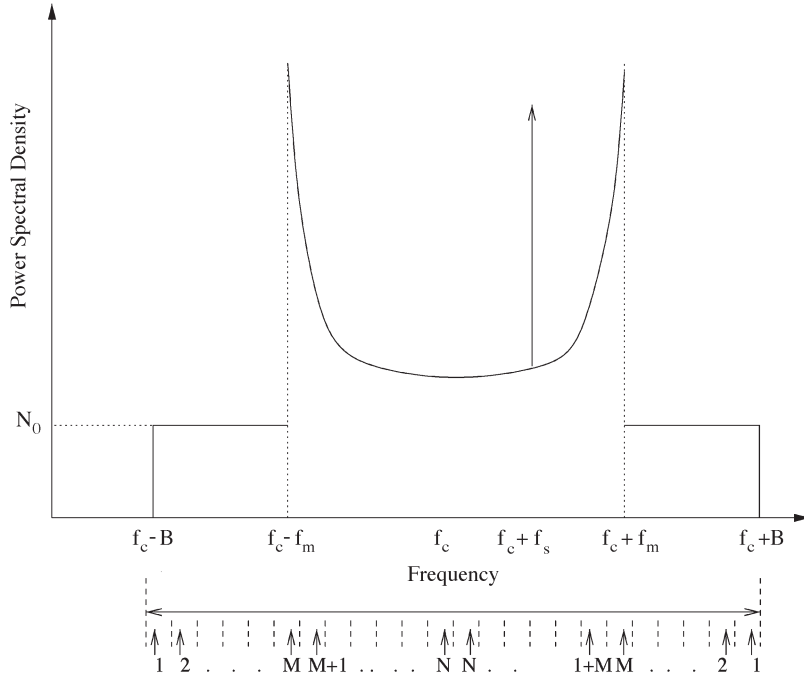


Fig. 1. PSD of the received signal envelope in a Rician fading channel in the presence of AWGN.

where  $\alpha_n$  is the amplitude of the  $n$ th arriving wave,  $\beta_{ns}$  are uniformly distributed over  $[-\pi, \pi]$ ,  $\theta_n$  is the angle of arrival of the  $n$ th arriving wave, and  $w(t)$  is the AWGN. For large  $N$ , the envelope of  $r(t)$ , i.e.,  $|r(t)|$  is Rayleigh distributed if no line-of-sight (LOS) component is present, else, it is Rician distributed.

In a Rician fading environment,  $S(f)$ , which is the power spectral density (PSD) of  $|r(t)|$ , is given in (3) (shown at the bottom of the page) [14] where  $\Omega$  is the total received envelope power,  $K$  is the Rice factor,  $N_0$  is the PSD of AWGN, and  $2B$  is the receiver bandwidth.  $f_s = f_c + f_m \cos \theta_0$  is the frequency of the LOS component where  $\theta_0$  is the angle of arrival of the LOS component. The plot of (3) is shown in Fig. 1. For a Rayleigh fading channel, i.e., a channel with no LOS component,  $S(f)$  can be derived from (3) when  $K = 0$ , and its plot is similar to Fig. 1, except that there is no LOS component. We differentiate (3) to get the slope of  $S(f)$  in a Rician fading

environment, which is given in (4) (shown at the bottom of the page). In (4), the slope has three maxima: 1) at  $f = f_c + f_m$ ; 2) at  $f = f_c - f_m$ ; and 3) at  $f = f_c + f_s$ . The maxima at  $f = f_c - f_m$  and  $f = f_c + f_m$  are due to the maximum Doppler frequency. The maximum at  $f = f_c + f_s$  is due to the LOS component. When the angle of LOS component  $\theta_0 = 0$ , the maximum of (4) due to  $f_m$  and  $f_s$  coincide with each other. Note that when no LOS component is present (Rayleigh fading channel), (4) has only two maxima: 1) at  $f = f_c + f_m$ ; and 2) at  $f = f_c - f_m$ . Therefore, for both Rayleigh and Rician fading, the slope of PSD of the received signal envelope has maximum values at frequencies of  $f_c \pm f_m$ . The frequency component,  $f = f_c + f_m$ , is always greater than or equal to  $f = f_c + f_s$  and greater than  $f = f_c - f_m$ . We detect the maximum value of (4), which corresponds to the highest frequency component ( $f_c + f_m$ ) to estimate  $f_m$ .

$$S(f) = \begin{cases} \frac{\Omega}{4(K+1)\pi f_m \sqrt{1 - (\frac{f-f_c}{f_m})^2}} + N_0, & |f - f_c| \leq f_m, f - f_c \neq f_s \\ \frac{\Omega}{4(K+1)\pi f_m \sqrt{1 - (\frac{f-f_c}{f_m})^2}} + \frac{K\Omega}{4(K+1)} + N_0, & f = f_c + f_s \\ N_0, & f_m < |f - f_c| < B \end{cases} \quad (3)$$

$$\frac{dS(f)}{df} = \begin{cases} \frac{\Omega(f-f_c)}{4(K+1)\pi f_m^3 [1 - (\frac{f-f_c}{f_m})^2]^{\frac{3}{2}}}, & |f - f_c| \leq f_m, f - f_c \neq f_s \\ \frac{\Omega(f-f_c)}{4(K+1)\pi f_m^3 [1 - (\frac{f-f_c}{f_m})^2]^{\frac{3}{2}}} + \frac{K\Omega}{4(K+1)} \delta(f_c + f_s), & f = f_c + f_s \\ 0, & f_m < |f - f_c| < fB \end{cases} \quad (4)$$

For practical implementation, we use discrete slope calculation. We divide the entire receiver bandwidth ( $2B$ ) into  $2N$  equally spaced intervals as shown in Fig. 1. Each interval has a mirror image about  $f_c$ . The discrete frequency value associated with the  $i$ th interval is  $f_c + B - (B/N)i$ . We calculate the slope as

$$S(k) = \frac{\sum_{i=1}^{k+1} P(i) - \sum_{i=1}^k P(i)}{2\Delta B} = \frac{P(k+1)}{2\Delta B} \quad (5)$$

where  $P(i)$  is the sum of the power of  $i$ th interval and its mirror image interval.  $\Delta B = B/N$  is the width of one interval. Using (5) and Fig. 1, it is clear that  $S(i)$ ,  $i = 1, 2, \dots, (M-2)$ , have the same value and are equal to the PSD  $N_0$  of AWGN. In a real scenario,  $N_0$  is not flat. Hence,  $S(i)$ ,  $i = 1, 2, \dots, (M-2)$ , are not exactly equal to each other. Their values are close to  $N_0$  and different from each other. When noise PSD ( $N_0$ ) is insignificant compared to the power in the interval containing frequency  $f = f_c + f_m$ ,  $S(M-1)$  will be dominant among all the slopes in a Rayleigh fading scenario. On the other hand, in a Rician fading scenario, the slopes corresponding to the intervals containing  $f_c + f_m$  and  $f_c + f_s$  are both dominant. However, the slope corresponding to the interval containing  $f_c + f_m$  is of lower order compared to the one corresponding to the interval containing  $f_c + f_s$ , where the order of the slope is given by  $k$  in (5). When both  $f_c + f_m$  and  $f_c + f_s$  belong to the same interval, there is only one dominant slope in case of a Rician fading scenario. We detect the lowest order dominant slope of the received signal envelope's PSD to estimate  $f_m$ . This ensures that our algorithm is independent of the fading environment.

The estimation of the lowest order dominant slope can be carried out in two ways, as follows: 1) calculate all the slopes and then detect the peak slope of lowest order; and 2) calculate  $S(1)$ , then  $S(2)$ , and so on until the first dominant slope is detected. In this approach, initially, the values of the slopes [ $S(1)$ ,  $S(2)$ , etc.] are close to  $N_0$  up to the slope corresponding to the interval containing  $f_c + f_m$ . The slope corresponding to interval containing  $f_c + f_m$  is significantly higher than  $N_0$ . This is the lowest order dominant slope. There is no need to calculate the other slopes.

For the second approach, there is no need to calculate all the slopes, and no sorting is required. Therefore, it has less computational complexity. However, it requires the knowledge about  $N_0$ . This requirement can be eliminated if the worst case signal-to-noise ratio (SNR) for a mobile system is known. If the value of  $N_0$  corresponding to worst case SNR is  $N_{0(\text{worst})}$ , then in the second approach, initially, the values of slopes corresponding to the intervals before the interval containing  $f_c + f_m$  are less than or equal to  $N_{0(\text{worst})}$ ; and the slope corresponding to the interval containing  $f_c + f_m$  is significantly higher than  $N_{0(\text{worst})}$ . Therefore, with the knowledge of  $N_{0(\text{worst})}$ , in the second approach, when a particular slope is significantly greater than  $N_{0(\text{worst})}$ , we consider that as the lowest order peak slope. We refer to  $N_{0(\text{worst})}$  as slope threshold  $S_{\text{th}}$  in the rest part of the paper. We use the second approach because of its

low computational complexity. If the lowest order peak slope corresponds to  $k = k_{\text{min}}$ , then

$$f_m = B - k_{\text{min}}(\Delta B). \quad (6)$$

To further reduce the computational complexity, we use a two-step approach to estimate  $f_m$ .

- 1) First, we carry out a coarse estimation of  $f_m = f_m^1$  using interval width of  $\Delta B_{\text{coarse}}$  for slope calculation in (5). If we denote the index of slope corresponding to lowest order peak as  $k_{\text{coarse}}$ ,  $f_m^1$  is expressed as

$$f_m^1 = B - k_{\text{coarse}}\Delta B_{\text{coarse}}. \quad (7)$$

- 2) Then, we carry out a finer estimate of  $f_m = \hat{f}_m$  using the interval of  $\Delta B$  for slope calculation in (5). In this step, we calculate the slope of the received signal envelope's PSD in the frequency range over  $f_m^1 - x$  to  $f_m^1 + x$ . Our choice of  $2x$  Hz over which the slope is calculated is arbitrary. Any value for  $x$  can be used as long as  $2x$  is greater than  $2\Delta B_{\text{coarse}}$  (which is the granularity of the previous step). If we denote the index of the peak slope, which has the lowest order as  $k_{\text{finer}}$ , then  $\hat{f}_m$  is given by

$$\hat{f}_m = f_m^1 + x - k_{\text{finer}}\Delta B. \quad (8)$$

Finally, we estimate the velocity using  $f_m = \hat{f}_m$  in (1). Equation (8) shows that, in VEPSD, the maximum error in velocity estimation ( $\Delta v$ ) is equal to the velocity corresponding to the Doppler spread of  $\Delta B$ , i.e.,  $\Delta v = \Delta B(c/f_c)$ . Thus, the error in estimation reduces as carrier frequency increases. Hence, our algorithm provides better estimation accuracy for the next generation of wireless systems that are expected to operate at higher carrier frequencies around 5 GHz. Another advantage of VEPSD is its scalability to estimate the velocity up to the desired level of accuracy through proper selection of the number of intervals ( $N$ ) for slope calculation. For example, to determine if the velocity of the mobile is slow, medium, or fast, we just need three intervals. On the other hand, using more number of intervals, an accurate estimation of the velocity can be achieved.

So far, we have discussed VEPSD for narrowband wireless communication systems. In case of code division multiple access (CDMA) systems, the mobile channel can be represented by the impulse response model [10]

$$h(\tau; t) = \sum_{k=1}^l h_k(t)\delta(\tau - kT_c) \quad (9)$$

where  $l$  is the number of resolvable paths,  $T_c$  is the chip interval, and  $h_k(t)$  is the complex channel gain of the  $k$ th multipath.  $h_k(t)$  has the form in (2) and  $|h_k(t)|$  is Rayleigh distributed when no LOS component is present, else, it is Rician distributed. The RAKE receiver can resolve each of the paths in (9) [16]. Then, the channel gain for the  $k$ th path,  $h_k(t)$ , can be obtained by the help of pilot channel or other means [11]. VEPSD uses this  $|h_k(t)|$  that contains the Doppler spreading information for velocity estimation. Hence, VEPSD works for CDMA systems as well.

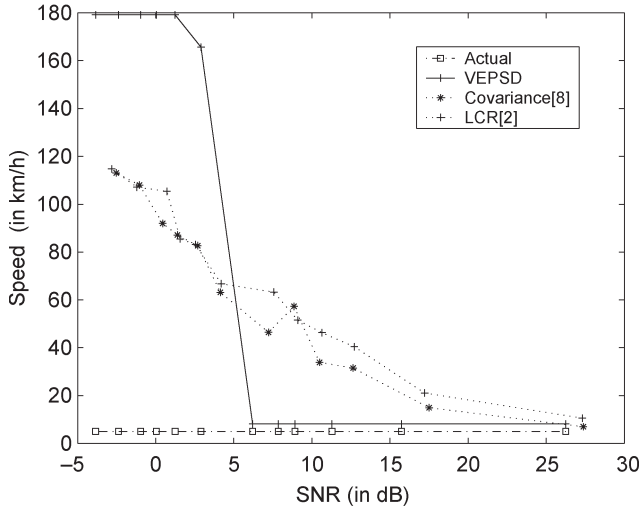


Fig. 2. Estimated velocity versus SNR in a Rayleigh fading channel for  $v = 5$  km/h with  $\tau = 1$  ms and  $T_{est} = 1$  s.

In case of multicarrier systems, the channel across each sub-carrier is a narrowband channel. Hence, the received signal envelope across any subcarrier can be used in VEPSD for velocity estimation.

Up until now, we discussed the algorithm for isotropic scattering environments. Nonisotropic scattering is usually modeled using von Mises/Tikhonov distribution [15]. Furthermore, in this case, the PSD of the received envelope has maximum values at frequencies  $f_c \pm f_m$ . Hence,  $f_m$  can be detected using our VEPSD algorithm. This ensures that the VEPSD algorithm is applicable to both isotropic and nonisotropic scattering environments.

### III. PERFORMANCE EVALUATION

We carried out the performance evaluation of the VEPSD algorithm through simulation. We selected the receiver bandwidth  $B$  such that it is just greater than the maximum Doppler spread for the highest vehicular velocity to minimize the effect of noise on estimation [2]. We consider  $B = 325$  Hz, which allows velocity up to 175 km/h at  $f_c = 2$  GHz. We use  $f_c = 2$  GHz, as this frequency band is widely used for cellular systems. We consider  $\Delta B = 5$  Hz that can estimate velocity to an accuracy of 2.7 km/h. We use  $\Delta B_{coarse} = 27$  Hz. To determine the value of the slope threshold  $S_{th}$ , we assume the worst case SNR to be 15 dB. This assumption is realistic as the typical SNR in cellular systems is in the order of 20 dB [8]. The threshold value is determined in such a way that  $S_{th} \gg N_0$ . This ensures that slight variation in  $N_0$  is not identified as a dominant slope. Through simulations, the value of  $S_{th}$  for coarse estimation (7) is found to be 20 and that for finer estimation (8) is 4.5. The estimation interval ( $T_{est}$ ) corresponds to the time interval over which the received signal envelope samples are collected for the velocity estimation. Hence,  $T_{est} = N\tau$ , where  $N$  is the number of samples and  $\tau$  is the sampling period. We use  $T_{est} = 1$  s and  $\tau = 1$  ms, because these values give a good estimate of the velocity.

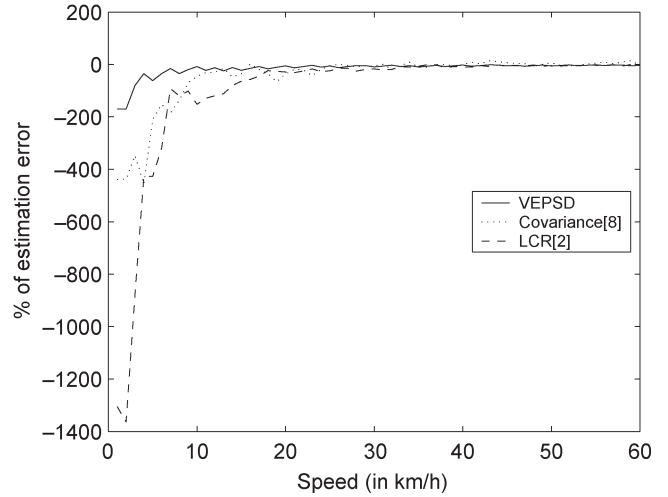


Fig. 3. Estimation accuracy in a Rayleigh fading channel for  $\tau = 1$  ms,  $T_{est} = 1$  s, and SNR = 20 dB.

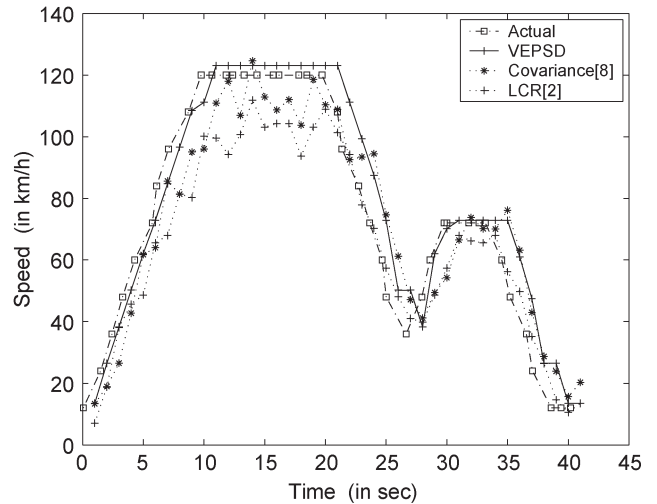


Fig. 4. Velocity tracking in a Rayleigh fading channel for  $\tau = 1$  ms,  $T_{est} = 1$  s, and SNR = 20 dB.

#### A. Simulation Results for a Rayleigh Fading Channel

We start with the investigation of the effect of AWGN on the estimation error in a Rayleigh fading channel. Then, we investigate the estimation accuracy for various ranges of velocity and analyze the response of the algorithm to changes in the velocity.

1) *Effect of AWGN on Accuracy of Velocity Estimation:* Fig. 2 shows the performance of the velocity estimation algorithms versus SNR for a velocity of 5 km/h. For VEPSD estimator, the performance is degraded when the SNR is below 7 dB in Fig. 2. This is because below these values, the relation  $S_{th} \gg N_0$  does not hold. Hence, the clear existence of the dominant value of the slope corresponding to frequency  $f_m$  is lost. From Fig. 2, it is clear that at very low SNR, the VEPSD algorithm always estimates the velocity to be 179 km/h. This is because for very low SNR,  $N_0 > S_{th}$ . Therefore, the VEPSD algorithm detects interval (1) as the interval corresponding to peak slope, both in coarse and fine estimation steps. Now, using (7) and (8),  $f_m$  is estimated as 331 Hz and the corresponding

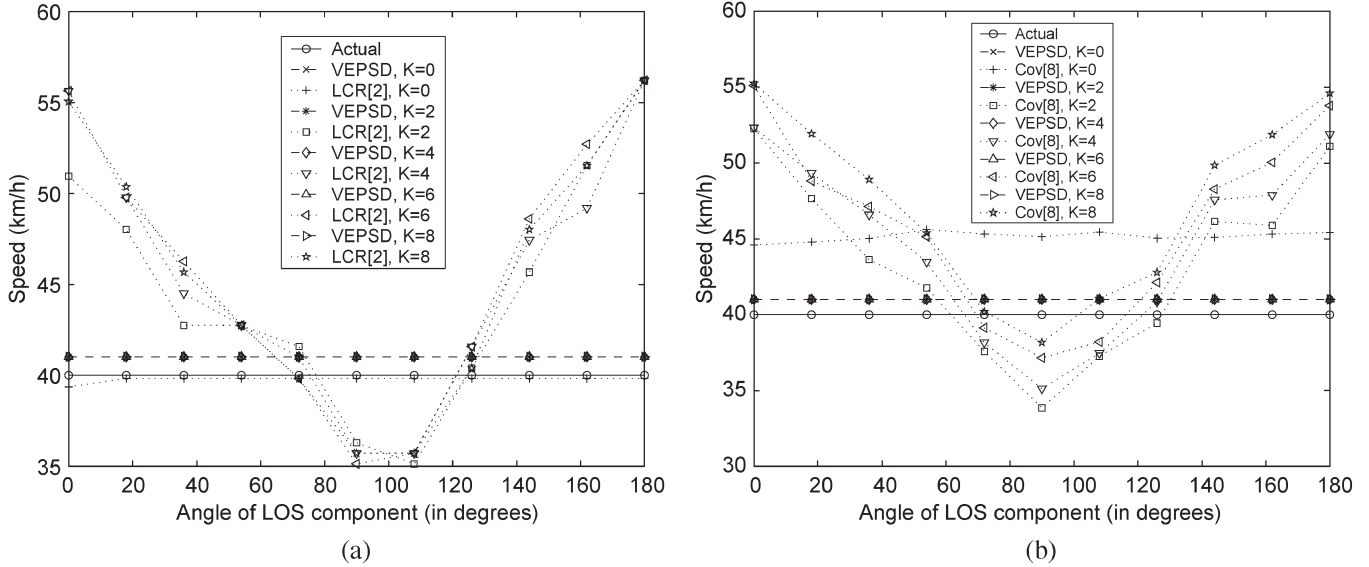


Fig. 5. Comparison of VEPSD estimator for  $v = 40$  km/h with  $\tau = 1$  ms,  $T_{est} = 1$  s, and SNR = 20 dB. (a) With LCR-based estimator. (b) With covariance-based estimator.

velocity is 179 km/h. Fig. 2 shows that the error in velocity estimation increases as the SNR decreases for both covariance and LCR-based methods. Furthermore, estimation error is severe for lower velocity compared to that for higher velocity for both LCR [2] and covariance [8]. Interestingly, the estimation error for VEPSD is independent of SNR when SNR is more than 10 dB for both low and high velocity values.

2) *Velocity Estimation Accuracy*: We carried out the simulation study for all the three estimation algorithms over the velocity range of 1–60 km/h. Fig. 3 shows that the proposed VEPSD algorithm can estimate the velocity to a very good accuracy over the entire range (1–60 km/h). This is in contrast to the LCR and the covariance-based estimators, where the error introduced by AWGN is severe for low velocity values.

3) *Velocity Tracking*: Fig. 4 shows that the tracking performance of all the three algorithms are comparable when the mobile is either accelerating or decelerating. When the mobile stays at a constant velocity, VEPSD has better accuracy of estimation than those of LCR-based [2] and covariance-based [8] estimators. This is because of the randomness of the received envelope, which varies the LCR count and also the variance from time to time. The VEPSD algorithm performs better in this case, because even for the randomly varying received envelope, the maximum Doppler frequency used by the VEPSD remains constant during each observation interval.

*B. Simulation Results for a Rician Fading Channel*

Fig. 5(a) and (b) shows that for VEPSD algorithm, the velocity estimation accuracy is independent of the angle of arrival of the LOS component ( $\theta_0$ ) and Rice factor ( $K$ ). This is in contrast to the covariance-based algorithm, where the accuracy of velocity estimation depends on  $K$  and  $\theta_0$  as shown in Fig. 5(b). The LCR-based estimator is robust to Rice factor ( $K$ ), when the level is chosen as the root mean square (rms) value of the received envelope samples. This also is clear from

Fig. 5(a), where the velocity estimation based on LCR depends only on the angle of arrival of the LOS component ( $\theta_0$ ) and is independent of the Rice factor. The robustness of VEPSD algorithm to  $K$  can be explained as follows. As  $K$  increases, the power of the LOS component increases and that of the scattered components decreases. But still, the nature of the PSD plot and, hence, its slope remains unchanged. Just that the value of slope decreases. For an SNR value greater than 15 dB, this value of slope is much greater than  $S_{th}$ . Therefore, the VEPSD algorithm still detects the peak corresponding to  $f_m$ . The value of  $\theta_0$  determines the position of the LOS frequency component ( $f_c \pm f_s$ ) with respect to  $f_c + f_m$ . However, our VEPSD algorithm always discards the peak value of slope at  $f_c \pm f_s$ , as discussed in Section II. Hence, it is insensitive to  $\theta_0$ .

IV. CONCLUDING REMARKS

In this paper, we presented velocity estimation using the power spectral density (VEPSD), a novel velocity estimation algorithm. We carried out a detailed performance analysis of the VEPSD algorithm and also compared it with two other existing algorithms, namely: 1) level crossing rate (LCR)-based velocity estimation [2]; and 2) covariance-based velocity estimation [8]. The results show that VEPSD algorithm works very well in both Rayleigh and Rician fading environments. The VEPSD algorithm is robust to both Rice factor and angle of arrival of the LOS component. This is the key advantage of VEPSD compared to LCR and covariance-based velocity estimators. We investigated the effect of additive white Gaussian noise (AWGN) on the accuracy of velocity estimation. The results show that VEPSD algorithm works significantly better in the signal-to-noise ratio (SNR) range typical of cellular systems. In addition, the tracking performance of the VEPSD estimator is comparable to other estimators. VEPSD algorithm works very well for wide range of velocities and is well suited for the next

generation of wireless systems operating at higher frequencies. VEPSD algorithm can be used to estimate velocity up to the desired level of accuracy. Hence, it is scalable.

#### ACKNOWLEDGMENT

The author acknowledges Prof. I. F. Akyildiz of the School of Electrical and Computer Engineering, Georgia Institute of Technology, Atlanta, GA, for all the useful discussions benefiting this paper.

#### REFERENCES

- [1] C. Xiao, K. D. Mann, and J. C. Olivier, "Mobile speed estimation for TDMA-based hierarchical cellular systems," *IEEE Trans. Veh. Technol.*, vol. 50, no. 4, pp. 981–991, Jul. 2001.
- [2] M. D. Austin and G. L. Stuber, "Velocity adaptive handoff algorithms for microcellular systems," *IEEE Trans. Veh. Technol.*, vol. 43, no. 3, pp. 549–561, Aug. 1994.
- [3] R. Narasimhan and D. C. Cox, "Speed estimation in wireless systems using wavelets," *IEEE Trans. Commun.*, vol. 47, no. 9, pp. 1357–1364, Sep. 1999.
- [4] K. Kawabata, T. Nakamura, and E. Fukuda, "Estimating velocity using diversity reception," in *Proc. IEEE Vehicular Technology Conf.*, Stockholm, Sweden, 1994, vol. 1, pp. 371–374.
- [5] T. L. Doumi and J. G. Gardiner, "Use of base station antenna diversity for mobile speed estimation," *Electron. Lett.*, vol. 30, no. 22, pp. 1835–1836, Oct. 1994.
- [6] L. Wang, M. Silventoinen, and Z. Honkasalo, "A new algorithm for estimating mobile speed at the TDMA-based cellular system," in *Proc. IEEE Vehicular Technology Conf.*, Atlanta, GA, 1996, pp. 1145–1149.
- [7] D. Mottier and D. Castelain, "A Doppler estimation for UMTS-FDD based on channel power statistics," in *Proc. IEEE Vehicular Technology Conf.*, Amsterdam, The Netherlands, 1999, pp. 3052–3056.
- [8] J. M. Holtzman and A. Sampath, "Adaptive averaging methodology for handoffs in cellular systems," *IEEE Trans. Veh. Technol.*, vol. 44, no. 1, pp. 59–66, Feb. 1995.
- [9] Y. Chung and D. Cho, "Velocity estimation using adaptive array antennas," in *Proc. IEEE Vehicular Technology Conf.*, Rhodes, Greece, 2001, pp. 2565–2569.
- [10] G. J. R. Povey, P. M. Grant, and R. D. Pringle, "A decision-directed spread-spectrum RAKE receiver for fast-fading mobile channels," *IEEE Trans. Veh. Technol.*, vol. 45, no. 3, pp. 491–502, Aug. 1996.
- [11] S. Min and K. B. Lee, "Channel estimation based on pilot and data traffic channels for DS/CDMA systems," in *Proc. IEEE Global Telecommunications Conf.*, Sydney, Australia, Nov. 1998, pp. 1384–1388.
- [12] G. Azemi, B. Senadji, and B. Boashash, "Velocity estimation in cellular systems based on the time–frequency characteristics of the received signal," in *Proc. Int. Symp. Signal Processing and Its Applications (ISSPA)*, Kuala Lumpur, Malaysia, Aug. 13–16, 2001, pp. 509–512.
- [13] W. Wang and I. F. Akyildiz, "On the estimation of user mobility pattern for location tracking in wireless networks," in *Proc. IEEE Global Telecommunications (GLOBECOM)*, Taipei, Taiwan, 2002, pp. 610–614.
- [14] G. L. Stuber, *Principles of Mobile Communication*, 2nd ed. Norwell, MA: Kluwer, 2001.
- [15] C. Tepedelenlioglu and G. B. Giannakis, "On velocity estimation and correlation properties of narrow-band mobile communication channels," *IEEE Trans. Veh. Technol.*, vol. 50, no. 4, pp. 1039–1052, Jul. 2001.
- [16] M. Turkboylari and G. L. Stuber, "Eigen-matrix pencil method-based velocity estimation for mobile cellular radio systems," in *Proc. IEEE Vehicular Technology Conf.*, New Orleans, LA, 2000, pp. 690–694.